Tightly coupled brain activity and cerebral ATP metabolic rate

Fei Du[†], Xiao-Hong Zhu[†], Yi Zhang[†], Michael Friedman[‡], Nanyin Zhang[†], Kâmil Uğurbil[†], and Wei Chen[†‡§]

[†]Department of Radiology, Center for Magnetic Resonance Research and [‡]Department of Biomedical Engineering, University of Minnesota Medical School, Minneapolis, MN 55455

Edited by Marcus E. Raichle, Washington University School of Medicine, St. Louis, MO, and approved March 18, 2008 (received for review November 13, 2007)

A majority of ATP in the brain is formed in the mitochondria through oxidative phosphorylation of ADP with the F_1F_0-ATP (ATPase) enzyme. This ATP production rate plays central roles in brain bioenergetics, function and neurodegeneration. *In vivo* ^{31}P magnetic resonance spectroscopy combined with magnetization transfer (MT) is the sole approach able to noninvasively determine this ATP metabolic rate via measuring the forward ATPase reaction flux ($F_{f,ATPase}$). However, previous studies indicate lack of quantitative agreement between $F_{f,ATPase}$ and oxidative metabolic rate in heart and liver. In contrast, recent work has shown that $F_{f,ATPase}$ might reflect oxidative phosphorylation rate in resting human brains. We have conducted an animal study, using rats under varied brain activity levels from light anesthesia to isoelectric state, to examine whether the *in vivo* ^{31}P MT approach is suitable for measuring the oxidative phosphorylation rate and its change associated with varied brain activity. Our results conclude that the measured $F_{f,ATPase}$ reflects the oxidative phosphorylation rate in resting rat brains, that this flux is tightly correlated to the change of energy demand under varied brain activity levels, and that a significant amount of ATP energy is required for ''housekeeping'' under the isoelectric state. These findings reveal distinguishable characteristics of ATP metabolism between the brain and heart, and they highlight the importance of *in vivo* ^{31}P MT approach to potentially provide a unique and powerful neuroimaging modality for noninvasively studying the cerebral ATP metabolic network and its central role in bioenergetics associated with brain function, activation, and diseases.

brain metabolism | *In vivo* ^{31}PMRS | ATPase | ATP synthesis | magnetization transfer

Adenosine triphosphate (ATP), a high-energy phosphate (HEP) compound, is the universal energy currency in living cells for supporting the energy needs of various cellular activities and functions. In the brain, a majority of ATP is formed in the mitochondria through oxidative phosphorylation of adenosine diphosphate (ADP) catalyzed by the enzyme of ATP synthase (ATPase) (1). A large portion of ATP energy is used in cytosol to pump sodium and potassium across the cellular membrane for maintaining transmembrane ion gradients and to support neurotransmitters cycling and, thus, sustaining electrophysiological activity and cell signaling in the brain. The ATP metabolism regulating both ATP production and utilization plays a fundamental role in cerebral bioenergetics, brain function, and neurodegenerative diseases (2–6).

The brain ATP metabolism is mainly controlled by ATPase and creatine kinase (CK) reactions that are coupled together and constitute a complex chemical exchange system involving ATP, phosphocreatine (PCr), and intracellular inorganic phosphate (Pi) (i.e., a PCr ⇄ ATP ⇄ Pi chemical exchange system) (7–10). One vital function of this ATP metabolic network is to maintain a stable cellular ATP concentration by adjusting the reaction rates to ensure a continuous energy supply for sustaining electrophysiological activity and maintaining normal function in the brain. Logically, both the kinetics of ATP metabolism and the associated chemical exchange rates should be more sensitive to the brain activity and energy states than the steady-state ATP concentration; they should provide an essential measure of cerebral bioenergetics under different brain activity states. The sole approach able to noninvasively and directly assess the cerebral ATP metabolic rates is *in vivo* ^{31}P magnetic resonance spectroscopy (MRS) combined with the magnetization transfer (MT) method (9–16).

The *in vivo* ^{31}P MT approach has significantly advanced the understanding of bioenergetics in the skeletal and cardiac muscles and brain, yet it has also been a catalyst of controversies regarding whether the measured ATP metabolic flux could truly reflect the rate of cerebral oxidative phosphorylation, which is expected to dominate the ATP production and bioenergetics. The ATP synthesis (i.e., Pi → ATP reaction) rate measured by the *in vivo* ^{31}P MT approach, in principle, can be mediated by many cellular processes involving this conversion. Most processes, however, are not fast enough relative to the intrinsic spin lattice time (T_1) of Pi to have a NMR detectable contribution. Surprisingly, the reactions catalyzed by glycolytic enzymes have been shown to be a major contributor to the Pi → ATP rate measured by the *in vivo* ^{31}P MT approach in *Escherichia coli* (17), yeast (18), liver (19), and myocardium (20). In the glucose perfused rat heart, the exchange mediated by the two coupled glycolytic enzymes of glyceraldehyde-3-phosphate dehydrogenase (GAPDH) and phosphoglycerate kinase (PGK) dominates the unidirectional *Pi → ATP* rate[¶] measured by the *in vivo* ^{31}P MT approach (20). This rate was shown to remain constant, whereas the myocardial oxygen consumption rate was approximately doubled under high workload. Only after the GAPDH/PGK contribution was eliminated, the Pi → ATP rate measured by the *in vivo* ^{31}P MT approach in the myocardium was found to match the rate of oxidative ATP synthesis rate (20).

The observations documenting the dissociation between the measured Pi → ATP rate and the oxidative ATP synthesis rate have diminished the significance of the *in vivo* ^{31}P MT approach for studying the cellular oxidative phosphorylation and its role in these biological systems. In contrast, we have recently demonstrated that the unidirectional Pi → ATP rate measured by the *in vivo* ^{31}P MT approach in the resting human brain was consistent with the oxidative ATP synthesis rate (9). This finding has led us to hypothesize that the *in vivo* ^{31}P MT approach could provide a unique and completely noninvasive tool for quantita-

Author contributions: F.D., X.-H.Z., K.U., and W.C. designed research; F.D., X.-H.Z., Y.Z., and W.C. performed research; M.F. and N.Z. contributed new reagents/analytic tools; F.D., X.-H.Z., Y.Z., N.Z., and W.C. analyzed data; and F.D., X.-H.Z., K.U., and W.C. wrote the paper.

The authors declare no conflict of interest.

This article is a PNAS Direct Submission.

§To whom correspondence should be addressed. E-mail: wei@cmrr.umn.edu.

¶In a reaction A ⇆ B, unidirectional rates are given as the rate of A → B or B → A, whereas the net rate is defined as the difference between the two unidirectional rates. The terms rate and flux are used interchangeably.

This article contains supporting information online at www.pnas.org/cgi/content/full/0710766105/DCSupplemental.

Table 1. Physiologic parameters of rats measured by blood gas analysis and *in vivo* ^{31}P MRS under four anesthesia conditions

Anesthesia condition	pCO_2, mm Hg	pO_2, mm Hg	C_{Glc}, mg/dl	ABP, mm Hg	HR, beats per min	pH	
						Blood	Tissue
IsoF	33.4 ± 2.9	141.5 ± 36.3	162.3 ± 14.4	103 ± 7	370 ± 25	7.49 ± 0.03	7.15 ± 0.01
α-Ch	31.0 ± 3.0	155.2 ± 20.2	112.0 ± 12.4*	108 ± 10	350 ± 33	7.43 ± 0.06	7.15 ± 0.02
Low-Pen	30.6 ± 2.8	131.6 ± 28.3	95.5 ± 15.3*	104 ± 13	394 ± 16	7.48 ± 0.05	7.16 ± 0.01
High-Pen	29.6 ± 4.8	156.0 ± 34.9	53.0 ± 6.0*	64 ± 6*	300 ± 14*	7.36 ± 0.03*	7.15 ± 0.04

The results were averaged from two blood samples collected before and after *in vivo* ^{31}P MT or EEG experiments under each physiological condition. The pH values of brain tissue were measured according to $pH = 6.75 + \log[(\delta - 3.26)/(5.70 - \delta)]$, where δ is the chemical shift difference between the P_i and PCr resonances. ABP, arterial blood pressure; HR, heart beating rate; C_{Glc}, blood glucose concentration.

*The measured parameter was statistically significant different ($P < 0.05$ with unpaired two-tailed *t* test) from that measured under the IsoF condition.

tively determining the oxidative ATP synthesis rate in the brain, which is vital for studying the cerebral bioenergetics and brain function (9). In the present study, we test this hypothesis and attempt to establish a noninvasive ^{31}P MRS approach for directly and quantitatively measuring the rate of oxidative phosphorylation and its change in the brain.

In vivo ^{31}P MT measurements, using the rat model, were performed at 9.4 tesla (T), concurrently with electroencephalogram (EEG) measurements under different brain activity levels attained by using varied anesthetics and/or anesthetic doses. Three essential questions were addressed herein: (*i*) Does the ATP synthesis rate measured by the *in vivo* ^{31}P MT approach reflect the cerebral oxidative phosphorylation rate? (*ii*) If it does, is it more sensitive to the change of brain activity than the steady-state HEP concentrations? (*iii*) If yes, what is the quantitative relationship between the cerebral oxidative phosphorylation rate and brain activity changes? The answers to these questions are important as a technical validation of *in vivo* ^{31}P MT approach in determining the cerebral oxidative phosphorylation rate and for understanding the neuro-metabolic coupling.

In this study, the rat brain activity was altered under four conditions by using three types of anesthetic chemicals [2% isoflurane (IsoF); α-chloralose (α-Ch), and sodium pentobarbital (Pen)], and two Pen doses (low-Pen vs. high-Pen) were applied, in which high-Pen led to complete suppression of spontaneous EEG signal (i.e., isoelectric state) (21). The *in vivo* ^{31}P MT approach (9–12) was applied to measure both the forward chemical exchange fluxes (F_f) from PCr to ATP [i.e., forward CK reaction flux ($F_{f,CK}$) related to the PCr → ATP reaction catalyzed by CK] and from P_i to ATP [i.e., forward ATPase reaction flux ($F_{f,ATPase}$) related to the Pi → ATP reaction catalyzed by ATPase] by selectively saturating the γ-ATP resonance peak under varied brain activity states in the rat. The rat brain activities were determined by EEG measurements and quantified by the spectral entropy index (SEI) based on the Shannon spectral entropy method (22). The details regarding the measurements of $F_{f,ATPase}$, $F_{f,CK}$, and SEI may be found in *Materials and Methods*.

Results

Animal Physiology. Significant efforts were made to maintain rats at normal and stable physiologic conditions. The relevant physiological parameters measured under four anesthesia conditions are summarized in Table 1. When anesthesia depth achieved by using α-chloralose or sodium pentobarbital increased, the blood glucose concentration (C_{Glu}) gradually and significantly decreased compared to the initial IsoF condition, and it reached the lowest level at the isoelectric state (high-Pen). The difference of C_{Glu} between the α-Ch and low-Pen conditions was statistically insignificant ($P > 0.05$ with unpaired two-tailed *t* test). From IsoF to high-Pen, a statistically significant but small difference in blood pH was noted, whereas the brain tissue pH remained constant. Other physiological parameters had not changed significantly under four anesthesia conditions except that arterial blood pressure and heart rate decreased 37 ± 9% and 19 ± 4%, respectively, at the isoelectric state compared with the IsoF condition.

Test of Independence of T_1 on Physiology Change. Because of the limited length of experimental time for performing multiple *in vivo* ^{31}P MT measurements in the same rat, the conventional saturation transfer (CST) approach with steady-state saturation of γ-ATP resonance peak was used to measure the ATP metabolic rates in the rat brains with three anesthesia conditions (group III: IsoF, low-Pen, and high-Pen; see details in *Materials and Methods*). By this approach, the unidirectional ATP reaction fluxes, $F_{f,ATPase}$ and $F_{f,CK}$, can be simultaneously deduced from two *in vivo* ^{31}P spectra acquired in the absence (control) and presence of the steady-state γ-ATP saturation according to Eq. **2**. However, the intrinsic spin lattice relaxation times of Pi ($T_{1,Pi}$) and PCr ($T_{1,PCr}$) in the absence of exchange with ATP have to be determined at a given magnetic field strength and are, in general, independent of the physiologic condition changes (9, 10). In this study, we have conducted a progressive saturation transfer experiments (see *Materials and Methods* and Eq. **1**) in the rat brain at 9.4T under the IsoF and α-Ch anesthesia conditions (i.e., groups I and II). Intrinsic $T_{1,PCr}$ (i.e., the T_1 of PCr in the absence of the PCr ⇆ ATP exchanges) was determined to be 3.68 ± 0.50 s for the IsoF condition and 3.97 ± 0.63 s for the α-Ch condition without a statistically significant difference ($P = 0.22$). Similarly, intrinsic $T_{1,Pi}$ was 4.17 ± 0.58 s and 3.89 ± 0.69 s for the IsoF and α-Ch condition ($P = 0.16$), respectively. These results indicate that both $T_{1,PCr}$ and $T_{1,Pi}$ are insensitive to the changes of animal physiology, and they can be treated as constant (9, 13, 23). Thus, the averaged $T_{1,PCr}$ (3.83 ± 0.57 s) and $T_{1,Pi}$ (4.03 ± 0.64 s) were used in the present study to calculate the forward chemical exchange rate constants for the steady-state saturation measurements according to Eq. **2**.

Coupling Between Varied Brain Activity and ATP Metabolic Rates. Fig. 1 shows typical *in vivo* ^{31}P MT spectra from a representative rat brain acquired in the absence (*Left*) and presence (*Center*) of the steady-state γ-ATP saturation under three anesthesia conditions (Fig. 1*A*, IsoF; Fig. 1*B*, low-Pen; and Fig. 1*C*, high-Pen). The corresponding EEG time courses measured in another rat are also illustrated in Fig. 1 (*Right*), showing a gradual decrease of brain EEG activity from the IsoF condition with burst EEG pattern to the isoelectric state with silent EEG activity.

The *in vivo* ^{31}P MT spectra shown in Fig. 1 clearly demonstrate a significant magnetization (or NMR signal) reduction in the PCr and P_i resonances due to the steady-state γ-ATP saturation and the magnetization transfer effect through the exchange reaction of PCr → ATP and Pi → ATP, respectively. The relative

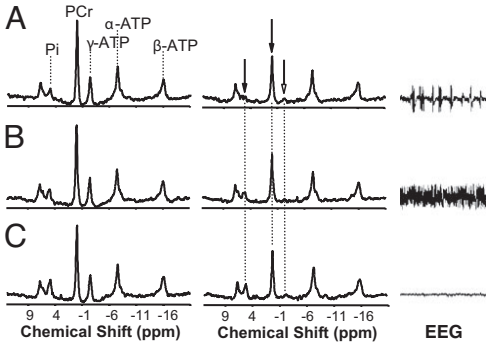

Fig. 1. *In vivo* ^{31}P MT and EEG measurements from a representative rat brain under IsoF (SEI = 0.75) (*A*), low-Pen (SEI = 0.65) (*B*), and high-Pen (isoelectric; SEI = 0.50) (*C*) anesthesia conditions, respectively. (*Left* and *Center*) ^{31}P spectra acquired in the absence (control) (*Left*) and presence (*Center*) of γ-ATP saturation. The magnetization ratio quantified by the NMR signals obtained at steady-state saturation versus control was 56%, 59%, and 63% for PCr and 59%, 67%, and 78% for Pi at IsoF, low-Pen, and high-Pen anesthesia conditions, respectively. The ratio changes indicate reduction in the measured ATP metabolic rates with increased anesthesia depth. (*Right*) EEG time courses recorded at three anesthesia conditions.

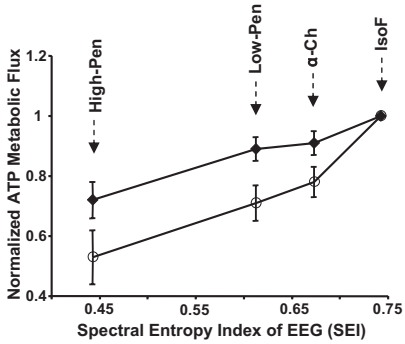

Fig. 2. Correlations between the averaged ATP metabolic rates of CK ($F_{f,CK}$ and full diamonds) and ATPase ($F_{f,ATPase}$ and open circles) reactions versus the averaged spectral entropy index of EEG measured under varied brain activity levels in the rat brain with four anesthesia conditions as labeled. Both $F_{f,CK}$ and $F_{f,ATPase}$ were normalized to the values measured under the IsoF condition.

magnetization reduction is proportional to the forward reaction rate constant according to Eq. **2**. It is evident that the unidirectional forward PCr → ATP and Pi → ATP rate constants (k_f) gradually decreased with increasing anesthesia depth. These constants and the Pi and PCr concentrations were used to calculate the forward unidirectional ATP reaction fluxes of $F_{f,ATPase}$ and $F_{f,CK}$ under the four anesthesia conditions according to Eq. **2**. These data are summarized in Table 2.

In general, all measured concentrations of [ATP], [PCr], and [Pi] were unaltered under IsoF, α-Ch, and low-Pen anesthesia conditions. Under the isoelectric state (i.e., high-Pen), however, we observed a decrease of 8 ± 2% in [PCr] and an increase of 42 ± 6% in [Pi] compared to the IsoF condition, whereas [ATP] still remained constant. The unidirectional reaction fluxes for PCr → ATP and Pi → ATP tended to decrease from the lightest (IsoF) to deepest (high-Pen) anesthesia conditions. A similar trend was consistently observed in the measured brain EEG activities (Table 2). The time domain EEG signal patterns and its entropy quantifications at four anesthesia conditions with various brain activity levels were similar to those reported in refs. 22 and 24. The general tendency of deepening anesthesia is to suppress both cerebral ATP metabolic activity and spontaneous brain EEG activity, which shifts the EEG signal to a lower-frequency domain and reduces the spectral entropy index.

Fig. 2 shows the relationship between the rat brain activity quantified by SEI versus the normalized ATP metabolic fluxes through the CK ($F_{f,CK}$) and ATPase ($F_{f,ATPase}$) reactions, respectively. The α-Ch and low-Pen anesthesia conditions did not induce a statistically significant difference ($P > 0.05$) in the values of $F_{f,CK}$ (59.5 ± 9.3 versus 58.4 ± 10.5), $F_{f,ATPase}$ (9.7 ± 1.2 versus 8.6 ± 1.0), and SEI (0.67 ± 0.04 versus 0.61 ± 0.03), indicating a similar anesthesia depth (or anesthetic effect) between these two conditions. In contrast, both the ATP metabolic rates and brain activities were significantly suppressed under the isoelectric state related to the IsoF condition, resulting in k_f and F_f decreases of 20 ± 8% and 28 ± 13% for the CK (i.e., PCr → ATP) reaction and 59 ± 17% and 48 ± 11% for the ATPase (Pi → ATP) reaction, respectively, and reducing the EEG spectral entropy index from 0.74 ± 0.06 to 0.44 ± 0.08.

Discussion

Brain ATP Energy Budget and "House-Keeping" Energy. In general, ≈90% of cerebral ATP production occurs in the mitochondria through oxidative phosphorylation (25). ATP utilization mainly occurs in the cytosol, providing chemical energy for supporting various cellular functions, including phospholipid metabolism, proteins synthesis, neurotransmitter cycling, and transportation of ions across cellular membranes. A significant amount of ATP energy budget in the brain is spent for maintaining and restoring the transmembrane Na^+/K^+ ion gradients that are diminished by neuronal firing associated with spontaneous brain activity (4, 25). At the isoelectric state, we observed that ≈50% of the oxidative ATP synthesis capacity relative to the lightly anesthetic state (i.e., IsoF condition) remained when EEG became silent. This result indicates that brain "house-keeping" activities and the spontaneous EEG activity under the IsoF condition each use approximately one-half of the total brain ATP energy as measured under the IsoF condition. It also suggests an important role of "house-keeping" ATP for maintaining cellular integrity in the brain.

Cerebral metabolic activity can be assessed experimentally by measuring the cerebral metabolic rates of oxygen ($CMRO_2$) and/or glucose (CMR_{glu}) consumption. These metabolic processes and their rates have been intensively studied by a variety of techniques, and their relationships to varied brain activity were investigated by using different anesthetics and doses (24, 26). The degree of CMR_{glc} suppression by deep pentobarbital anesthesia was reported to be 40–60% compared with nitrous

Table 2. Measurements of ATP energy metabolism and brain activity under four varied anesthesia conditions

Anesthesia Condition	PCr, mM	ATP, mM	P_i, mM	$k_{f,CK}$, s^{-1}	$k_{f,ATPase}$, s^{-1}	$F_{f,CK}$, μmol/g/min	$F_{f,ATPase}$, μmol/g/min	EEG SEI
IsoF	5.0	3.0	1.3	0.24 ± 0.02	0.17 ± 0.03	65.4 ± 7.3	12.1 ± 1.9	0.74 ± 0.06
α-Ch	4.99 ± 0.21	3.03 ± 0.21	1.28 ± 0.13	0.21 ± 0.03*	0.13 ± 0.02*	59.5 ± 9.3	9.7 ± 1.2*	0.67 ± 0.04*
Low-Pen	4.95 ± 0.14	3.05 ± 0.15	1.26 ± 0.17	0.21 ± 0.02*	0.12 ± 0.02*	58.4 ± 10.5	8.6 ± 1.0*	0.61 ± 0.03*
High-Pen	4.60 ± 0.29*	2.98 ± 0.10	1.85 ± 0.19*	0.19 ± 0.03*	0.07 ± 0.03*	46.8 ± 10.0*	6.4 ± 1.9*	0.44 ± 0.08*

*The measured parameter was statistically significant different ($P < 0.05$ with unpaired two-tailed *t* test) from that measured under the IsoF condition.

oxide analgesia, light α-chloralose anesthesia, or the conscious animal (24, 27, 28). It was also reported that administration of sodium pentobarbital reduced CBF and $CMRO_2$ by 66% and 61%, respectively, relative to a light anesthetic condition with morphine sulfate (21). Other reports showed that thiopental-induced isoelectric condition resulted in a reduction of global $CMRO_2$ and CMR_{glc} by 47% and 61%, respectively, in the non-human primate brain relative to the awake condition (29, 30). The range of 40–61% reduction in the brain metabolic rates as found in these reports is in line with the reduction of ≈50% in the forward unidirectional ATPase reaction flux measured in our study, indicating a significant ATP consumption for "house-keeping" under the isoelectric condition. However, caution should be practiced when quoting the "house-keeping" energy as a percentage of the total brain energy budget, because the latter depends on the selection of the reference brain state (or baseline level). For instance, ≈35% reduction in $CMRO_2$ was reported in the dog brain under anesthesia with 2% end-tidal isoflurane concentration compared to an awake state (31). Thus, the "house-keeping" ATP requirement at the isoelectric state measured in our study would become ≈33% in comparison with that in the awake brain, consistent with the concept that the majority of ATP energy is used to support brain activity and neuronal signaling in the resting and conscious brain (4–6).

Although the majority of ATP is produced in neurons via the oxidative phosphorylation of ADP, there is considerable oxidative ATP synthesis in the glia cells based on *in vivo* ^{13}C MRS studies (6, 27, 28). The fraction of brain energy consumption between neuron and glia cells will change with varied brain activity; and substantial energy consumption in the glia cells has been reported under deep pentobarbital anesthesia or isoelectric conditions (6, 27, 28). The agreement between the ATPase reaction flux measurement in the present study and other measurements of total oxygen or oxidative glucose consumption as a function of brain activity suggests that the forward ATPase reaction flux measured by the *in vivo* ^{31}P MT approach might be contributed from both neuron and glia cells; although the glia contribution is relatively small, in most cases, it could become significant under the isoelectric state.

Coupling Among Forward ATPase Reaction Flux, Oxidative Phosphorylation, and Brain Activity. Oxygen and glucose are the two most important exogenous substrates for supporting brain energy and function. The majority of brain glucose is oxidatively metabolized. Under physiological conditions, oxidative metabolism is tightly coupled with the oxidative phosphorylation process that produces ATP molecules from Pi and ADP through the mitochondrial ATPase. This metabolic pathway can produce 15 times more ATP molecules than the glycolysis pathway. Thus, the oxidative glucose metabolism associated with the oxygen utilization dominates the ATP production in the brain. Moreover, the high energy demand in the brain requires correspondingly high rates of ATP production and utilization, resulting in fast chemical cycling among ADP and Pi versus ATP. The net rate of oxidative ATP synthesis in this cycling is given as the product of $2 \times$ (P:O ratio) $\times$ $CMRO_2$. The unidirectional rate of ATP synthesis measured by the ^{31}P MT approach can be equal to or greater than this rate. In all organs examined except in the brain, unidirectional rate of ATP synthesis measured by ^{31}P MT (i.e., $F_{f,ATPase}$) exceeded net rate of oxidative ATP synthesis substantially. The notable exception has been the brain as founded by previous measurements in the resting human brain from our group and previous rat brain studies in refs. 9, 10, and 13. This surprising finding was further examined in the present study under the conditions in which we have performed rigorous $CMRO_2$ measurements, using high-field ^{17}O MRS, ultimately, to test whether $F_{f,ATPase}$ determined by ^{31}P MT changed as brain energy demand was altered.

First, we examined the relationship between the $F_{f,ATPase}$ value measured in this study and the net oxidative phosphorylation rate calculated from the P:O ratio and the $CMRO_2$ value, assuming a tight coupling between the oxidative phosphorylation and oxygen utilization (3–6, 9, 10). We had determined the $CMRO_2$ value to be 2.2 $\mu mol \cdot g^{-1} \cdot min^{-1}$ in the rat brain (32) under the same α-chloralose anesthesia condition (i.e., α-Ch condition) used in the current study. Multiplication of this $CMRO_2$ value with $2\times$ P:O ratio with a P:O ratio of 2.4 (20, 33) yields a rate of 10.6 $\mu mol \cdot g^{-1} \cdot min^{-1}$ for net ATP synthesis by oxidative phosphorylation, in excellent agreement with $F_{f,ATPase}$ values of 9.7 ± 1.2 $\mu mol \cdot g^{-1} \cdot min^{-1}$ measured by ^{31}P MT under the same animal condition in this study. This result further validates the conclusion reached in the awake human brain (9, 10) and in the rat brain with sodium pentobarbital anesthesia (13). The significance of the current data are particularly important, because the $CMRO_2$ and $F_{f,ATPase}$ were examined under identical experimental conditions, albeit in different animals, thus removing potential sources of error in the comparison. In addition, the 50% reduction in $F_{f,ATPase}$ measured by ^{31}P MT under the isoelectric state compared to light anesthetic state in this study was in excellent agreement with the 40–61% reduction of $CMRO_2$ reported. This indicates that $F_{f,ATPase}$ remains approximately proportional to the $CMRO_2$ value across a wide range of brain activity. Consistent with this conclusion, our results also demonstrate that with increasing anesthesia depth, $F_{f,ATPase}$ decreased progressively (Table 1 and Fig. 1), and its reduction was parallel to the decreased EEG activity as quantified by SEI, revealing a tight neurometabolic correlation between the oxidative ATP production rate measured by the *in vivo* ^{31}P MT approach and the brain activity level assessed by EEG.

This study clearly demonstrates that a close relationship between $F_{f,ATPase}$ and the level of brain activity can be extended from the resting brain to a wide range of brain activity levels from awaked human brain to the rat brain with complete suppression of spontaneous EEG. In contrast, such a relationship is lacking in the heart, because the measured $F_{f,ATPase}$ in myocardium is dominated by the glycolytic enzyme activities (20). The cellular mechanism for understanding this discrepancy between the brain and heart is still unclear (9, 10). However, the measurement of $F_{f,ATPase}$ relies on the Pi signal reduction induced by the saturation of γ-ATP resonance peak and the magnetization transfer effect between Pi and γ-ATP; it is possible that the Pi signal detected by *in vivo* ^{31}P MRS in the brain may mainly anticipate the Pi $\rightarrow$ ATP reaction through the oxidative, rather than glycolytic, pathway; thereby, the measured $F_{f,ATPase}$ largely reflects the majority of ATP production through oxidative phosphorylation in the brain mitochondria (9, 10). However, the exact mechanism requires further investigation, using cell cultures of neuron and astrocyte.

Coupling Between CK Reaction Flux and Brain Activity. The high energy demand in the brain results in fast chemical cycling among cellular ATP, ADP, and Pi, which requires rapid energy transportation between the cytosol and mitochondria. This can be accomplished by PCr through the reversible CK reactions that can facilitate the effective transport of ATP from mitochondria to sites of energy utilization and vice versa for ADP (8, 23). Thus, a close coupling between the CK reaction flux and the brain activity level could exist in a wide range of brain activity levels. Such a neuro-metabolic coupling between $F_{f,CK}$ and SEI was examined in this study and shown in Fig. 2. In comparison with $F_{f,ATPase}$, the measured unidirectional CK reaction flux was relatively less sensitive to the different brain activity levels. This is not unexpected, because $F_{f,CK}$ exceeds $F_{f,ATPase}$ by fivefold (Table 2) under all conditions in this study, consistent with reports in refs. 9, 10, and 13. These results reveal that the PCr

and CK reaction have a supportive role in the cerebral ATP metabolism.

HEP and Pi Concentrations vs. Brain Energy and Activity Changes. Although the steady-state concentrations of cellular HEP and Pi are closely linked to the cerebral ATP metabolism and are vulnerable to brain pathology, they are relatively stable and insensitive to brain energy demand and its change under physiological conditions. This notion is clearly evident in this study, showing a very stable brain ATP concentration under four anesthesia conditions (Table 2) despite an ≈50% reduction in the oxidative ATP production rate in the rat brain at the isoelectric state related to the light isoflurane anesthesia condition. Thus, the cerebral ATP metabolic rate should logically provide a more sensitive and accurate measure for quantifying brain energetics and its change under different brain activity states compared to the steady-state ATP concentration.

The ADP concentration and/or the ratio of [Pi]/[PCr] are commonly used to reflect the oxidative metabolic activity and bioenergetic level in the tissues under steady-state conditions. They were found to increase significantly in the human skeletal muscle during exercise (34, 35) and in the rabbit brain under a prolonged epileptic condition (36) owing to higher energy demand. One of the surprising findings from our study is the observation of increases in [Pi]/[PCr] and [ADP] under the isoelectric condition with high dose of pentobarbital anesthesia, which presents a minimal level of metabolic and brain activity. We found that [PCr] decreased 8 ± 2% and [Pi] increased 42 ± 6% at the isoelectric state compared with the light isoflurane anesthesia condition without detectable variation in pH and [ATP] (Tables 1 and 2). These changes result in an increase of 55% in [Pi]/[PCr] and 17% in [ADP]; the latter was calculated by assuming that the creatine kinase reaction remained at equilibrium during these two conditions and that the [PCr] is approximately one-half of the total creatine concentration in the brain. It had been shown that severe brain stress, such as hypoxia or ischemia, could also lead to a large increase in both [ADP] and [Pi]/[PCr] (36). To exclude this possibility, we have conducted a localized *in vivo* ^{1}H MRS experiment to examine whether the brain cellular lactate concentration, a common indicator of hypoxia, increased under the isoelectric condition. Supporting information (SI) Fig. S1 demonstrates the spectra acquired in a representative rat brain under three anesthesia conditions (IsoF, low-Pen, and high-Pen), showing no sign of significant lactate increase under the isoelectric condition. This result excludes the possible contribution of hypoxia to the increased [ADP] and [Pi]/[PCr] under the isoelectric state as observed in our study. It is, thus, possible that, under the isoelectric condition, V_{max} for oxidative ATP synthesis decreases and that corresponding increases in ADP and P_i contents are required to maintain an equilibrium balance between ATP production and utilization.

Summary. The following conclusions may be drawn from this study: (*i*) the forward unidirectional ATPase reaction flux measured by the *in vivo* ^{31}P MT approach reflects the net oxidative ATP synthesis rate in the brain; (*ii*) this flux is highly correlated to brain energy demands at different brain activity levels; and (*iii*) the cerebral ATP metabolic rate, which can be explicitly and noninvasively determined by the *in vivo* ^{31}P MT approach, would provide a more sensitive and quantitative measure of brain bioenergetics and its change associated with brain activity change under physiological condition compared with the steady-state HEP and Pi concentrations. These compelling findings reveal distinguishable characteristics of ATP metabolism between the brain and other organs. They also highlight the importance of the *in vivo* ^{31}P MT approach in studying the central roles of oxidative ATP metabolism in cerebral bioenergetics, brain function, and neurodegenerative diseases.

Materials and Methods

Animal Preparation. Male Sprague–Dawley rats (260–350 g body weight) were divided into four study groups (9–14 rats for each group). In group I, rats were anesthetized via inhalation of 2% (vol/vol) isoflurane in the nitrous oxide/oxygen (3:2) mixture. In group II, rats were anesthetized by α-chloralose with a 40 mg/kg bolus followed by continuous infusion (25 mg·kg^{-1}·h^{-1}). *In vivo* ^{31}P MT measurements, using the progressive saturation method (9–12), were performed for both groups I and II to measure (*i*) the intrinsic spin lattice relaxation times of Pi and PCr and (*ii*) the forward rate constants and fluxes for the $P_i \rightarrow$ ATP and PCr → ATP reaction, respectively.

In group III, rats were anesthetized under three conditions: (*i*) For IsoF, by inhalation of 2% (vol/vol) isoflurane in the nitrous oxide/oxygen (3:2) mixture; (*ii*) for low-Pen, by switching from IsoF condition to sodium pentobarbital with a 30 mg/kg bolus followed by continuous infusion (30 mg/kg/h); and (*iii*) for high-Pen, by increasing the sodium pentobarbital infusion rate to 70 mg·kg^{-1}·h^{-1} to achieve an isoelectric state ≈40 min after the high-dose infusion. *In vivo* ^{31}P MT measurements, using the steady-state saturation method (9–12), were performed for group III to measure the forward rate constants and fluxes for the $P_i \rightarrow$ ATP and PCr → ATP reactions, respectively, under the three anesthesia conditions.

In group IV, rats were anesthetized under the four aforementioned anesthesia conditions: IsoF, α-Ch, low-Pen, and high-Pen. This group was used for EEG measurements with the same protocol used for the *in vivo* ^{31}P MT experiments.

All *in vivo* ^{31}P MT and EEG measurements were performed after animal physiology approached a stable condition. The residue concentration of isoflurane was controlled to remain <0.1% (vol/vol) for the measurements under α-chloralose or sodium pentobarbital anesthesia conditions. Usually it took ≈90 min to switch anesthetics from isoflurane to α-chloralose or sodium pentobarbital. The femoral artery and vein were catheterized for blood sampling, physiology monitoring, and infusing α-chloralose or sodium pentobarbital solutions. Animal rectal temperatures were maintained at 37 ± 1°C throughout the experiments. All surgical procedures and experimental protocols were according to the guidelines of the National Institutes of Health and approved by the Institutional Animal Care and Use Committee of the University of Minnesota.

***In Vivo* ^{31}P MT Measurements.** All *In vivo* ^{31}P MT experiments were conducted on a 9.4T horizontal animal magnet (Magnex Scientific) interfaced to a Varian INOVA console. A multinuclear radiofrequency (RF) surface-coil probe consisting of a butterfly-shape ^{1}H surface coil and an elliptical-shape ^{31}P surface coil with axes of 12 mm and 10 mm were used. The ^{1}H surface coil was used to acquire brain anatomy imaging and for shimming magnetic field homogeneity, using the FASTMAP autoshimming algorithm (37). The ^{31}P detection sensitivity was crucial for reliably measuring the small Pi signal and its change caused by the MT effect to determine the oxidative ATP production rate (9, 10). To achieve maximal ^{31}P NMR sensitivity, the spatial localization of *in vivo* ^{31}P MRS for acquiring the rat brain signal was achieved by the local detection sensitivity profile defined by the ^{31}P RF surface coil without the use of other localization techniques. We have conducted a ^{31}P chemical shift imaging study to ensure that the Pi contribution from the muscle surrounding the brain was negligible (Fig. S2), suggesting that the measured Pi signal and $F_{f,ATPase}$ were mainly attributed to the rat brain tissue. The cortical gray matter likely dominated the contribution because of favorable detection sensitivity and the very small volume ratio of white mater to gray matter of <0.14 in the rat (38) (see *SI Materials and Methods*).

There are two saturation methods in performing the MT experiments. One is the progressive saturation transfer measurements with a variable saturation time (*t*) at near fully relaxed condition and then performing a curve fitting according to Eq. **1** (9, 10):

$$M_a(t) = M_a^0 \left(\frac{k_f}{k_f + T_{1a}^{-1}} e^{(k_f + T_{1a}^{-1})t} + \frac{1}{k_f T_{1a} + 1} \right) \qquad [1]$$

where *a* stands for PCr or Pi resonance peak; $M_a(t)$ and M_a^0 are the resonance magnetizations measured with the saturation time of *t* and $t = 0$, respectively; k_f is the pseudo-first-order forward rate constant; and T_{1a} is the intrinsic spin lattice relaxation time of Pi ($T_{1,Pi}$) or PCr ($T_{1,PCr}$). Both k_f and T_{1a} values can be determined by the regression analysis of Eq. **1**. The second saturation method is the use of a sufficiently long saturation of γ-ATP resonance for reaching a

steady-state of PCr or Pi magnetization (M_a^0). In this case, k_f and the forward unidirectional ATP reaction fluxes can be determined by Eq. **2**:

$$k_f = \frac{M_a^0 - M_a^*}{M_a^* T_{1a}}; \quad F_{\mathrm{f,ATPase}} = k_{\mathrm{f,ATPase}}[Pi]; \quad F_{\mathrm{f,CK}} = k_{\mathrm{f,CK}}[\mathrm{PCr}]. \qquad [2]$$

The pulse sequence used for the *in vivo* ^{31}P MT experiments in this study is described in refs. 9 and 10. For the progressive saturation experiments, the γ-ATP resonance was selectively saturated with varied saturation time. For the steady-state saturation experiments, a long saturation time of 6.6 s was used to achieve steady-state magnetizations for both PCr and Pi. The ^{31}P spectra were acquired under approximately fully relaxed condition (repetition time, 9 s) with other acquisition parameters of 512 data points, a 5,000-Hz spectral width, and 128 signal averages. The quantification of the HEP metabolites was based on the assumption of [PCr] = 5.0 mM, [ATP] = 3.0 mM, and [P_i] = 1.3 mM under the IsoF condition as reported in refs. 2, 9, 13, and 23. The HEP and Pi concentrations under other anesthesia conditions were calculated from their PCr, γ-ATP, or P_i signal integrals relative to that measured under the IsoF condition.

EEG Measurements. Two electrodes were used to record EEG signals from the rat brain (group IV). One was put on the rat nose to served as a reference, and the tip of the other was inserted into the rat cortex (2 mm deep from the surface of skull, 3 mm posterior to bregma, and 3 mm from the brain midline) through a small hole in the skull. The filtered EEG signal (0.0–30 Hz) was sampled at a rate of 1,000 Hz, using commercially available EEG equipment (Grass Instruments). Home-made software based on the Shannon spectral entropy method (22) was used to quantify EEG data and to calculate the spectral entropy index (SEI $\leq$ 1), where a high SEI value indicates a high brain activity level. The EEG signal was divided into epochs of 10-s duration, and then the spectral entropy index was calculated for each epoch in the 0.3- to 30-Hz frequency range. The reported EEG spectral entropy index value was obtained by averaging 20 min data acquired under each physiological condition.

Statistical Analysis. Unpaired two-tailed *t* tests were applied to statistical analysis of the experimental data. The results are presented as mean $\pm$ SD.

ACKNOWLEDGMENTS. This work was in part supported by National Institutes of Health Grants NS39043, NS41262, P41 RR08079, and P30 NS057091 and the W. M. Keck Foundation.

1. Boyer PD (1999) What makes ATP synthase spin? *Nature* 402:247–249.
2. Erecinska M, Silver IA (1989) ATP and brain function. *J Cereb Blood Flow Metab* 9:2–19.
3. Clarke DD, Sokoloff L (1999) in *Basic Neruochemistry: Molecular, Cellular and Medical Aspects*, eds Siegel GJ, *et al.* (Lippincott-Raven, Philadephia), pp 633–669.
4. Attwell D, Laughlin SB (2001) An energy budget for signaling in the grey matter of the brain. *J Cereb Blood Flow Metab* 21:1133–1145.
5. Raichle ME, Mintun MA (2006) Brain work and brain imaging. *Annu Rev Neurosci* 29:449–476.
6. Hyder F, *et al.* (2006) Neuronal-glial glucose oxidation and glutamatergic-GABAergic function. *J Cereb Blood Flow Metab* 26:865–877.
7. Slater EC, Holton FA (1953) Oxidative phosphorylation coupled with the oxidation of alpha-ketoglutarate by heart-muscle sarcosomes. I. Kinetics of the oxidative phosphorylation reaction and adenine nucleotide specificity. *Biochem J* 55:530–544.
8. Kemp GJ (2000) Non-invasive methods for studying brain energy metabolism: What they show and what it means. *Dev Neurosci* 22:418–428.
9. Lei H, Ugurbil K, Chen W (2003) Measurement of unidirectional Pi to ATP flux in human visual cortex at 7 T by using *in vivo* ^{31}P magnetic resonance spectroscopy. *Proc Natl Acad Sci USA* 100:14409–14414.
10. Du F, Zhu XH, Qiao H, Zhang X, Chen W (2007) Efficient *in vivo* ^{31}P magnetization transfer approach for noninvasively determining multiple kinetic parameters and metabolic fluxes of ATP metabolism in the human brain. *Magn Reson Med* 57:103–114.
11. Forsen S (1963) Study of moderately rapid chemical exchange reactions by means of nuclear magnetic double resonance. *J Chem Phys* 39:2892–2901.
12. Brown TR, Ugurbil K, Shulman RG (1977) ^{31}P nuclear magnetic resonance measurements of ATPase kinetics in aerobic Escherichia coli cells. *Proc Natl Acad Sci USA* 74:5551–5553.
13. Shoubridge EA, Briggs RW, Radda GK (1982) ^{31}P NMR saturation transfer measurements of the steady state rates of creatine kinase and ATP synthetase in the rat brain. *FEBS Lett* 140:289–292.
14. Ugurbil K (1985) Magnetization-transfer measurements of individual constants in the presence of multiple reactions. *J Magn Reson* 64:207–219.
15. Degani H, Alger JR, Shulman RG, Petroff OA, Prichard JW (1987) ^{31}P magnetization transfer studies of creatine kinase kinetics in living rabbit brain. *Magn Reson Med* 5:1–12.
16. Spencer RG, Balschi JA, Leigh JS, Jr, Ingwall JS (1988) ATP synthesis and degradation rates in the perfused rat heart. ^{31}P-nuclear magnetic resonance double saturation transfer measurements. *Biophys J* 54:921–929.
17. Mitsumori F, Rees D, Brindle KM, Radda GK, Campbell ID (1988) ^{31}P-NMR saturation transfer studies of aerobic *Escherichia coli* cells. *Biochimica et Biophysica Acta* 969:185–193.
18. Campbell SL, Jones KA, Shulman RG (1987) ^{31}P NMR saturation-transfer measurements in *Saccharomyces cerevisiae*: Characterization of phosphate exchange reactions by iodoacetate and antimycin A inhibition. *Biochemistry* 26:7483–7492.
19. Thoma WJ, Ugurbil K (1987) Saturation-transfer studies of ATP-Pi exchange in isolated perfused rat liver. *Biochimica et Biophysica Acta* 893:225–231.
20. Kingsley-Hickman PB, *et al.* (1987) ^{31}P NMR studies of ATP synthesis and hydrolysis kinetics in the intact myocardium. *Biochemistry* 26:7501–7510.
21. Hyder F, *et al.* (2000) Dependence of oxygen delivery on blood flow in rat brain: A 7 tesla nuclear magnetic resonance study. *J Cereb Blood Flow Metab* 20:485–498.
22. Bruhn J, Lehmann LE, Ropcke H, Bouillon TW, Hoeft A (2001) Shannon entropy applied to the measurement of the electroencephalographic effects of desflurane. *Anesthesiology* 95:30–35.
23. Sauter A, Rudin M (1993) Determination of creatine kinase kinetic parameters in rat brain by NMR magnetization transfer. Correlation with brain function. *J Biol Chem* 268:13166–13171.
24. Koga K, Miura I (1988) A measurement of cerebral glucose uptake rate by ^{31}P MRS. *Biochem Biophys Res Commun* 157:1258–1263.
25. Rolfe DF, Brown GC (1997) Cellular energy utilization and molecular origin of standard metabolic rate in mammals. *Physiol Rev* 77:731–758.
26. Sokoloff L (1981) Relationships among local functional activity, energy metabolism, and blood flow in the central nervous system. *Fed Proc* 40:2311–2316.
27. Choi IY, Lei H, Gruetter R (2002) Effect of deep pentobarbital anesthesia on neurotransmitter metabolism *in vivo*: On the correlation of total glucose consumption with glutamatergic action. *J Cereb Blood Flow Metab* 22:1343–1351.
28. Oz G, *et al.* (2004) Neuroglial metabolism in the awake rat brain: CO_2 fixation increases with brain activity. *J Neurosci* 24:11273–11279.
29. Nemoto EM, Klementavicius R, Melick JA, Yonas H (1996) Suppression of cerebral metabolic rate for oxygen ($CMRO_2$) by mild hypothermia compared with thiopental. *J Neurosurg Anesthesiol* 8:52–59.
30. Nemoto EM, Yao L, Yonas H, Darby JM (1994) Compartmentation of whole brain blood flow and oxygen and glucose metabolism in monkeys. *J Neurosurg Anesthesiol* 6:170–174.
31. Stullken EH, Jr, Milde JH, Michenfelder JD, Tinker JH (1977) The nonlinear responses of cerebral metabolism to low concentrations of halothane, enflurane, isoflurane, and thiopental. *Anesthesiology* 46:28–34.
32. Zhu XH, *et al.* (2002) Development of ^{17}O NMR approach for fast imaging of cerebral metabolic rate of oxygen in rat brain at high field. *Proc Natl Acad Sci USA* 99:13194–13199.
33. Hinkle PC (2005) P/O ratios of mitochondrial oxidative phosphorylation. *Biochim Biophys Acta* 1706:1–11.
34. Chance B, *et al.* (1985) Control of oxidative metabolism and oxygen delivery in human skeletal muscle: A steady-state analysis of the work/energy cost transfer function. *Proc Natl Acad Sci USA* 82:8384–8388.
35. Chance B, *et al.* (1986) Multiple controls of oxidative metabolism in living tissues as studied by phosphorus magnetic resonance. *Proc Natl Acad Sci USA* 83:9458–9462.
36. Prichard JW, Alger JR, Behar KL, Petroff OA, Shulman RG (1983) Cerebral metabolic studies *in vivo* by ^{31}P NMR. *Proc Natl Acad Sci USA* 80:2748–2751.
37. Gruetter R (1993) Automatic, localized *in vivo* adjustment of all first- and second-order shim coils. *Magn Reson Med* 29:804–811.
38. Zhang K, Sejnowski TJ (2000) A universal scaling law between gray matter and white matter of cerebral cortex. *Proc Natl Acad Sci USA* 97:5621–5626.